Geophysical Research Letters®

Key Points:

- Correction term for skin temperature (ΔT) from reanalysis products is consistent with that derived from field measurements
- ΔT is dominated by the cool skin effect except in certain regions such as near the equator where the warm layer effect is significant
- The correction could lead to -1%–$+36\%$ difference in annual air-to-sea O_2 flux and -33%–$+5\%$ difference in annual net community production

Skin Temperature Correction for Calculations of Air-Sea Oxygen Flux and Annual Net Community Production

Bo Yang[1,2] , Steven R. Emerson[3] , and Meghan F. Cronin[4]

[1]Rosenstiel School of Marine and Atmospheric Science, Cooperative Institute for Marine and Atmospheric Studies, University of Miami, Miami, FL, USA, [2]NOAA Atlantic Oceanographic and Meteorological Laboratory (AOML), Miami, FL, USA, [3]School of Oceanography, University of Washington, Seattle, WA, USA, [4]NOAA Pacific Marine Environmental Laboratory (PMEL), Seattle, WA, USA

Abstract We evaluated the influence of skin temperature correction on the calculations of air-sea O_2 flux and annual net community production (ANCP). The skin temperature correction term (ΔT) was derived from the fifth generation European Center for Medium-Range Weather Forecasts Reanalysis, which has large spatial and temporal variations that are consistent with independent measurements on three ocean moorings from areas with very different air-sea heat flux and ΔT. The result revealed that ΔT is dominated by the cool skin effect (which leads to the increase in air-to-sea O_2 flux and decrease in ANCP), except for the equatorial region or summertime when the warm layer effect is significant. Using data from three Argo profiling floats in the subarctic, subtropical, and tropical Pacific as examples, the calculations indicated that the correction could lead to -1%–$+36\%$ difference in annual air-to-sea O_2 flux and -33%–$+5\%$ difference in ANCP.

Plain Language Summary The skin of the ocean can be slightly cooler than the surface mixed layer due to net surface heat loss (cool skin effect), or slightly warmer due to extreme solar radiation (warm layer effect). We used the fifth generation European Center for Medium-Range Weather Forecasts Reanalysis (ERA5) to derive the skin temperature correction term (ΔT) for calculating the air-sea O_2 flux and the annual net carbon export (annual net community production, ANCP). ΔT derived from ERA5 has large spatial and temporal variations, and is consistent with independent measurements on three ocean moorings from areas with very different air-sea heat flux and ΔT. The result showed that ΔT is mostly dominated by the cool skin effect (which leads to the increase in air-to-sea O_2 flux and decrease in ANCP), except for the equatorial region or summertime when the warm layer effect is significant. Calculations using data from three profiling floats in the subarctic, subtropical, and tropical Pacific indicated that the correction could lead to -1%–$+36\%$ difference in annual air-to-sea O_2 flux and -33%–$+5\%$ difference in ANCP.

1. Introduction

Air-sea gas flux calculations rely on knowing the difference between gas concentrations measured in the mixed layer and the expected values based on equilibrium with the atmosphere. Therefore, different choices of temperature values used for the calculation can lead to large difference in both regional and global scale estimates of air-sea gas flux (e.g., Watson et al., 2020).

Because turbulent air-sea heat fluxes and net longwave radiation act upon the skin of the ocean (~500 μm, Donlon et al., 2002), while solar radiative fluxes penetrate below the surface, the skin of the ocean is nearly always slightly cooler than the surface mixed layer water below the skin (Hasse, 1963). The cool skin temperature difference across the thermal skin (referred to here as the "skin layer") can vary spatially and seasonally due to processes that control the wind stress and surface heat loss, including sea surface temperature, air-sea temperature difference, and wind speed (Fairall et al., 1996). Based on the in-situ infrared radiometer measurements in the Atlantic Ocean, Donlon et al. (1999) suggested a mean cool skin effect of $\Delta T_{cool} = -0.14 \pm 0.1$ K (negative sign means the surface skin is cooler). This value was later updated with additional measurements in the Pacific Ocean to a global estimate of $\Delta T_{cool} = -0.17 \pm 0.07$ K (Donlon et al., 2002). ΔT_{cool} has also been derived with surface mooring data (e.g., air/water temperature, solar radiation, humidity) using boundary layer heat flux models (e.g., COARE 3.0, Fairall et al., 2003).

Another factor that affects the surface ocean temperature gradient is the diurnal warm layer, which occurs during the day under low wind conditions when the temperature stratification caused by solar radiation suppresses

near-surface turbulent mixing, causing significant warming (ΔT_{warm}) in the upper few meters of the ocean (Donlon et al., 2007; Fairall et al., 1996). The residence time of O_2 in the surface mixed layer with respect to air-sea exchange is on the order of weeks to a month and that for CO_2 is roughly 10 times longer (Yang et al., 2019) because of reactions among the constituents of dissolved inorganic carbon (DIC = HCO_3^- + CO_3^{2-} + CO_2). Therefore, with the exception of where diurnal warming rectifies into longer time scales (i.e., during summertime in regions of very weak winds or in low-wind regions of the tropics), in most cases the cool skin effect is more impactful than the warm layer effect on the air-sea O_2 and CO_2 fluxes.

Although the magnitude of the cool skin effect on air-sea gas exchange is open to some question (e.g., McGillis & Wanninkhof, 2006) because of the different molecular diffusion coefficients of heat and mass, the cool skin correction has been widely accepted and repeatedly applied to air-sea CO_2 flux studies (e.g., Goddijn-Murphy et al., 2015; Watson et al., 2020; Woolf et al., 2016). A global mean cool skin effect of − 0.17 K (Donlon et al., 2002) results in "an increased net CO_2 flux in to the oceans by 0.8–0.9 PgC yr^{-1}, at times doubling the uncorrected values" (Watson et al., 2020). However, the warm layer effect has not yet been evaluated for the calculation of air-sea gas exchange.

In the past two decades, technology has made it possible to obtain long-term, in-situ O_2 records from autonomous platforms like Argo profiling floats. The time-series O_2 data from Argo floats has been increasingly used to determine the upper ocean Net Community Production (NCP), which is defined as net primary production minus community respiration, an important metric to quantify the marine biological carbon export (e.g., Bushinsky & Emerson, 2015; Riser & Johnson, 2008; Yang et al., 2019). Among the fluxes necessary for calculating the upper ocean O_2 mass balance, the most important terms are usually the air-sea O_2 flux and O_2 production from NCP (Yang et al., 2018), indicating the importance of air-sea gas exchange to the determination of the rate of biologically produced O_2.

In this work we focus on: (a) creating a data set of skin temperature correction terms with realistic spatial and temporal variations; (b) evaluating the correction terms against the that derived from field data at three time-series surface moorings (Cronin et al., 2006, 2015); and (c) determining the influence of skin temperature correction on air-sea O_2 fluxes and ANCP calculations, using O_2 data from Argo profiling floats.

2. Methods

2.1. Skin Temperature Correction Term Derived From Reanalysis Products

The European Center for Medium-Range Weather Forecasts Reanalysis v5 (ERA5, https://cds.climate.copernicus.eu/cdsapp#!/dataset/reanalysis-era5-single-levels?tab=form) is an atmospheric reanalysis of the global climate covering the period from 1950 to present, which provides hourly estimates of a large number of atmospheric, land and oceanic climate variables with a spatial resolution of 0.25° (Hersbach et al., 2018).

We use the daily mean of the difference between ERA5 T_{skin} and SST (ΔT, Equation 1) as the correction term (Luo & Minnett, 2020). The ERA5 SST is a "foundation" SST (i.e., the SST that is free from daily variations due to the diurnal cycle of the sun) taken from the blended in situ and satellite operational SST and Sea Ice Analysis (Donlon et al., 2012). The ERA5 skin temperature (T_{skin}) takes both cool skin and diurnal warm layer into account (IFS Documentation CY47R1, 2020).

$$\Delta T = T_{warm} + T_{cool} = T_{skin} - SST \qquad (1)$$

To obtain the ΔT value for a mooring or Argo float on a specific day, the gridded daily ΔT field was spatially interpolated to the specific mooring or Argo location. Because the SST measured by the SOS-Argo float is at 4–10 m at night, it can be considered comparable to the ERA5 SST.

2.2. Skin Temperature Correction Term Derived From Surface Mooring Measurements

The ΔT derived from field measurements at three long-term surface moorings were used to validate the ERA5-derived ΔT. ΔT estimates at these moorings were computed using COARE 3.0b algorithm (Fairall et al., 2003) with the mooring-measured parameters (e.g., radiation, air temperature, seawater temperature, wind speed, relative humidity, etc.). The surface mooring data (Cronin et al., 2006, 2015) from Ocean Station Papa (OSP, 50.1°N,
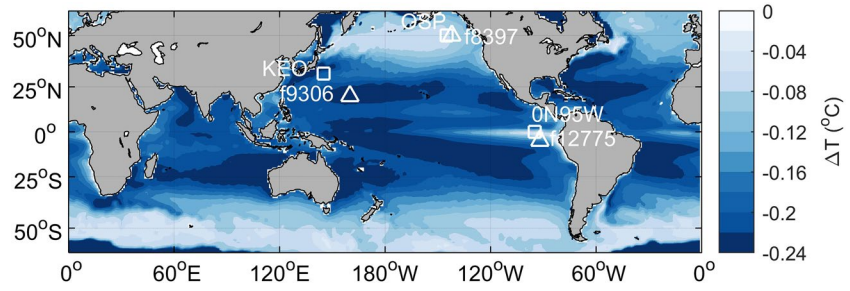
Figure 1. Annual mean (2014–2020) skin temperature correction (K) for extrapolating sea surface temperature to the skin temperature, derived from fifth generation European Center for Medium-Range Weather Forecasts Reanalysis products. The squares and triangles indicate locations of surface moorings (Ocean Station Papa, Kuroshio Extension Observatory, and 0N95W) and Argo profiling floats (f8397, f9306, and f12775), respectively.

144.9°W), Kuroshio Extension Observatory (KEO, 32.3°N, 144.6°E), and equatorial Pacific (0N95 W, 0°N, 95°W) were chosen (white squares in Figure 1), because they represent a wide range of surface forcing and ΔT values. The daily mean of T_{skin} and SST from OSP, KEO and 0N95 W were from https://www.pmel.noaa.gov/ocs/data/fluxdisdel/, https://www.pmel.noaa.gov/tao/drupal/disdel/, and Cronin et al. (2006).

2.3. Air-Sea O_2 Flux Calculation for Argo Float Measurements

Oxygen, salinity, and temperature data from Special Oxygen Sensor Argo floats (SOS-Argo, https://sites.google.com/a/uw.edu/sosargo/home) f8397, f9306, and f12775 were chosen in correspondence with the three mooring sites (subarctic, subtropical, and equatorial), to demonstrate the influence from skin temperature correction on air-sea O_2 flux and ANCP calculations. It should be noted that because there was no SOS-Argo in the equator where the warm layer effect is significant, we used the ΔT at 0N, 95W for the nearby float f12775 (5S, 100W) for demonstration purpose. These floats operated at a profiling cycle of 5–10 days, covering depths from 4 to 1,800 m with a vertical resolution of 3–5 m in the top 200 m of the water column. The air-calibrated Aanderaa® optode O_2 sensors on these SOS-Argo floats were capable of providing the air-sea difference in O_2 concentration with an accuracy better than ±0.2% (Bushinsky et al., 2016).

The air-sea O_2 flux (F_{A-S}, mol O_2 m^{-2}d^{-1}) is calculated using the model described by Liang et al. (2013) and Emerson and Bushinsky (2016) as amended by Emerson et al. (2019), in which both fluxes from diffusion (F_S) and bubble injection (F_B) are considered (Equation 2).

$$F_{A-S} = F_S + F_B \tag{2}$$

The driving force for the diffusion flux of oxygen, F_s, is the air-sea oxygen concentration difference (defined as positive from the air to the ocean).

$$F_s = k_s \cdot ([O_2]_{sat} - [O_2]) \tag{3}$$

$[O_2]$ is the measured seawater oxygen concentration in surface mixed layer, and $[O_2]_{sat}$ is the concentration of oxygen at the air-sea interface in saturation equilibrium with the pO_2 of the atmosphere calculated using solubility values determined from temperature and salinity (Garcia & Gordon, 1992, 1993). When the surface mixed layer $[O_2]$ is higher than the saturation value, O_2 diffuses out of the ocean and therefore F_s is negative. Here we argue that because both k_s (mass transfer coefficient for air-sea gas diffusion) and $[O_2]_{sat}$ are temperature-dependent, the diffusive flux of oxygen across the air-sea interface, F_S, should be estimated using the skin temperature rather than the SST.

The bubble flux F_B includes fluxes from small and large bubbles (F_c and F_p, respectively). The O_2 added into the ocean by F_c depends only upon wind stress and is independent of temperature since small bubbles collapse and completely dissolve in the water. In contrast, large bubbles exchange gases with the surrounding seawater, a process which is temperature dependent. But since this occurs well below the skin of the ocean, the temperature used for F_p is the mixed layer temperature and therefore doesn't need to be corrected. Details of air-sea O_2 flux calculation can be found in Emerson and Bushinsky (2016) and the Supporting Information S1.

2.4. Net Community Production Calculation With Argo O_2 Data

An O_2 mass balance model described in our previous work (Bushinsky & Emerson, 2015; Yang et al., 2018) was used to compute the NCP and annual NCP (ANCP) for SOS-Argo floats. Briefly, the net biological oxygen production (F_{NCP}) is determined as the difference between the observations (d (hO_2)/dt: Oxygen inventory changes with time in a depth domain of the winter mixed layer depth, h) and the physical processes that influence the oxygen concentration (F_{A-S}: air-sea exchange, F_w: vertical advection, F_{Kz}: diapycnal eddy diffusion).

$$\frac{d[hO_2]}{dt} = F_{A-S} + F_{NCP} + F_w + F_{Kz} \tag{4}$$

F_{NCP} can be converted to NCP with a constant oxygen to carbon ratio of 1.45 (Hedges et al., 2002).

3. Results and Discussion

The spatial distribution of the ERA5-derived annual mean ΔT (Figure 1) indicates that the correction is strong between 32°S and 35°N, and weaker at higher latitudes and the equator. Competing processes make a simple explanation of the global ΔT patterns. The impact of winds on the microlayer, latent and sensible heat loss and SST (and thus longwave radiative heat flux) leads to a cool skin that tends to be larger in low wind regions and smaller in high wind regions (Zhang et al., 2019). However, in tropics and summer seasons of high latitude regions, the diurnal warm layer can be significant where winds are weak (e.g., eastern equatorial Pacific). The large spatial variations (Figure 1) and significant deviations from the fixed correction term of −0.17 K (Figure S1 in Supporting Information S1) suggests that it is not suitable to use a fixed correction term for discrete air-sea gas flux estimate in different regions.

To explore the seasonality of ΔT and evaluate the performance of the ERA5-derived ΔT we compared the ΔT derived from ERA5 products to the skin temperature minus bulk SST measurements at OSP/KEO moorings from 2014 to 2020 and 0N95 W mooring from 2000 to 2003. For OSP and KEO (Figures 2a and 2b), the negative ΔT indicates the skin temperature correction is dominated by the cool skin effect. Since the bulk SST measured at 1.2 m on occasion show diurnal variability, these measured bulk SST are within the diurnal warm layer and the buoy ΔT does not capture the full diurnal warming relative to the foundation SST. The relatively good agreement with the ERA5 ΔT thus suggests that the ERA5 might underestimate the diurnal warm layer. In general, for a given region, ΔT (cooling) is stronger in the winter (further from zero) and weaker in the summer (closer to zero), consistent with larger surface heat loss in the winter and a more significant warm layer effect during the summertime. At OSP (Figure 2a), ΔT was mostly between 0 and −0.15 K, with the weakest effect between May and September. The type II linear regression between ΔT values derived from ERA5 and field data at OSP is presented in Figure 2d, with $y = (0.90 \pm 0.01) x + (−0.01 \pm 0.001)$, $R = 0.97$, and RMSD = 0.009 K. ΔT was significantly stronger at KEO, ranging from −0.40 K in the winter (mid-November) to near-zero in June (Figure 2b). The type II linear regression result at KEO was slightly worse than that at OSP, with $y = (0.83 \pm 0.02) x + (−0.05 \pm 0.005)$, $R = 0.88$, and RMSD = 0.04 K (Figure 2e). At the equational site 0N95 W (Figure 2c), ΔT had occasional positive values from January to May, and more consistent negative values at other times, consistent with the observations from Cronin and Kessler (2002). The result of type II linear regression at 0N95 W is significantly worse (Figure 2f), with $y = (0.69 \pm 0.09) x + (0.0002 \pm 0.009)$, $R = 0.36$, and RMSD = 0.11 K, which indicates that the ERA5 reanalysis may need some fine tunings for that equatorial region where the warm layer effect is significant. The comparison in Figure 2 indicates that: (a) The ERA5-derived ΔT was generally consistent with that derived from the mooring data over a wide range of ΔT values; (b) ΔT is mostly dominated by the cool skin effect (which leads to negative ΔT), although the warm layer effect is likely underestimated by both mooring measurements and ERA5 reanalysis; and (c) the warm layer effect was largest at the eastern equatorial site.

Air-sea O_2 fluxes (F_{A-S}) calculated using oxygen data from three Argo floats with and without the skin temperature correction are presented in Figure 3. The results are presented in the form of monthly F_{A-S}, to retain information about seasonal variations while the differences in F_{A-S} values caused by the cool skin/warm layer effect can be clearly shown. For float f8397, ΔT was between −0.05 and −0.1 K throughout the year (Figure 3a). For float f9306, ΔT was between −0.2 and −0.3 K throughout the year (Figure 3c). For float f12775, ΔT was between −0.05 and +0.11 K with both positive and negative values appeared (Figure 3e). The difference between F_{A-S}
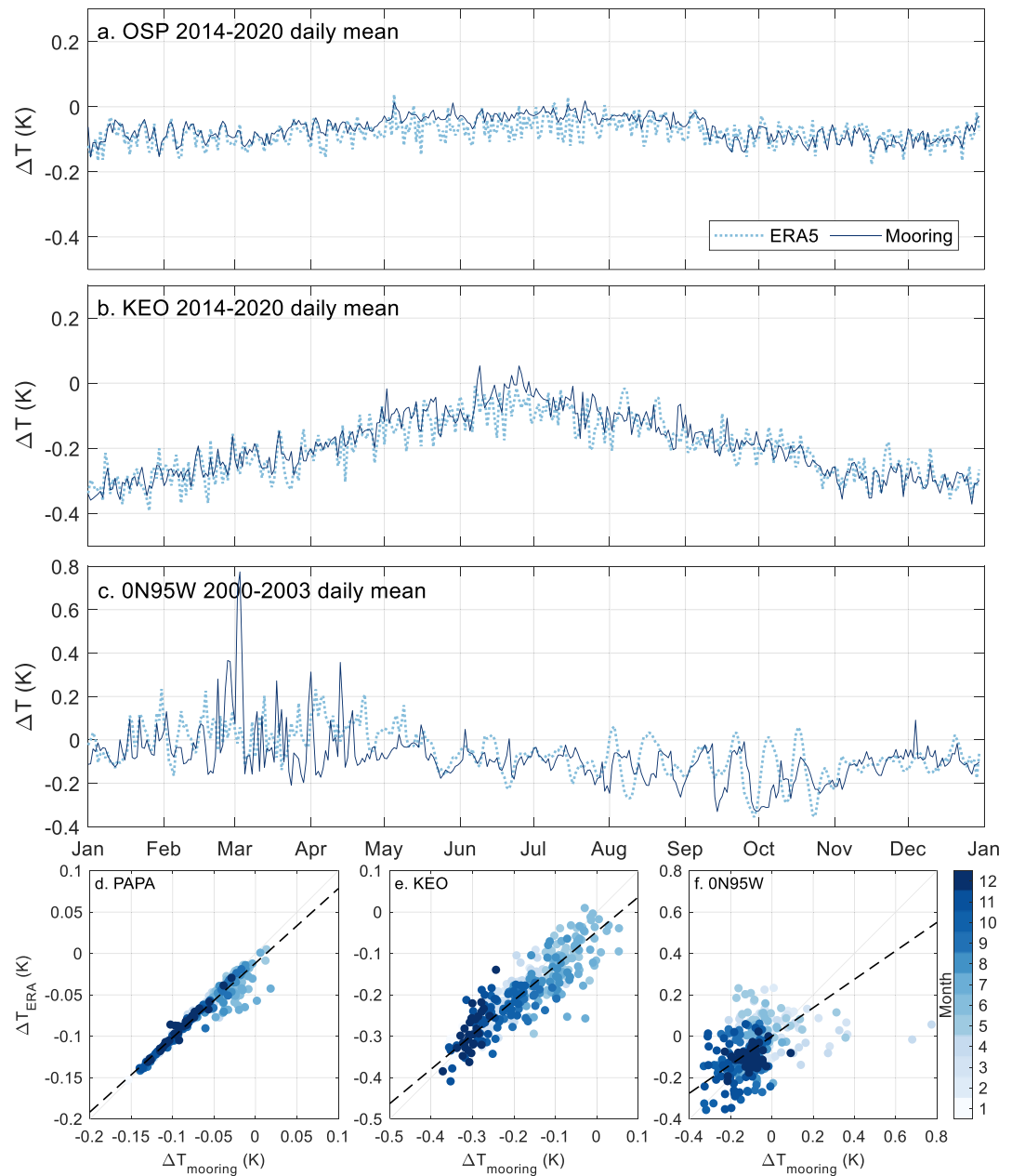
Figure 2. Comparison of temperature correction (ΔT, K) derived from fifth generation European Center for Medium-Range Weather Forecasts Reanalysis (ERA5) product and mooring measurements (a–c): daily mean values of ΔT at Ocean Station Papa, Kuroshio Extension Observatory, and 0N95W (d–f): Type II linear regressions of ΔT determined from the ERA5 product and the mooring measurements. The gray diagonal line is 1:1 line, and the black dash line presents the regression line.

calculated with and without correcting for skin temperature is significant. When ΔT is negative (ΔT dominated by cool skin effect, e.g., Figure 3a) it decreases the skin temperature and colder water contains more gas at atmospheric equilibrium. When F_{A-S} is positive (O_2 flux from the atmosphere to the ocean), the cooler skin temperature enhances the air-to-sea oxygen flux (e.g., January in Figure 3b); when F_{A-S} is negative (O_2 flux from the ocean to the atmosphere), the cooler skin temperature decreases the sea-to-air O_2 flux (e.g., June in Figure 3b). In contrast, when ΔT is positive (ΔT dominated by warm layer effect, e.g., Figure 3e) it increases the skin temperature and warmer water contains less gas at atmospheric equilibrium. When F_{A-S} is positive, the warmer skin temperature reduces the air-to-sea oxygen flux (e.g., May to August in Figure 3f); when F_{A-S} is negative, the warm layer effect
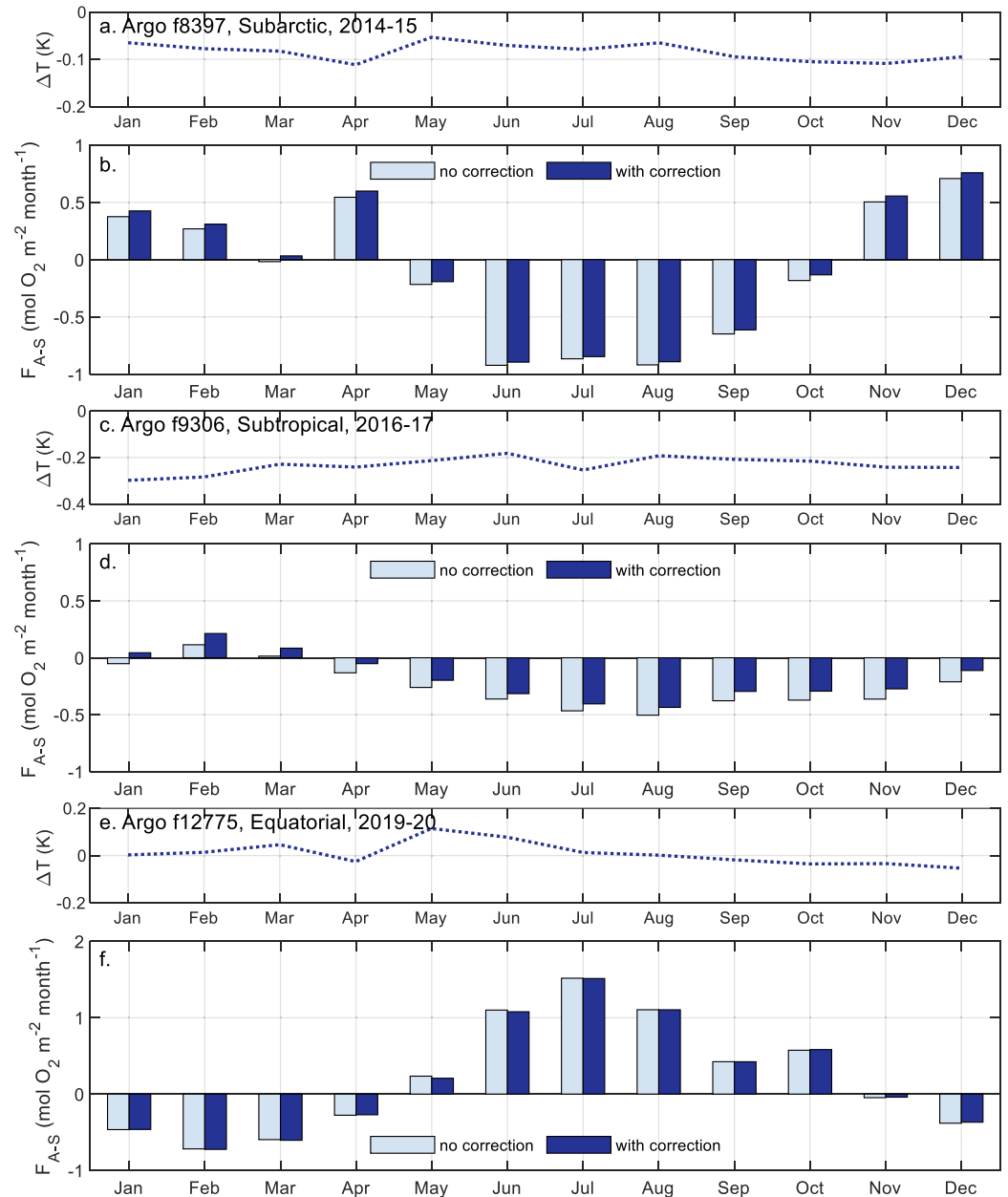
Figure 3. (a, c, and e): The temperature correction (k) derived from fifth generation European Center for Medium-Range Weather Forecasts Reanalysis products (b, d, and f): Monthly air-sea O_2 flux (F_{A-S}, mol O_2 m^{-2} month^{-1}) calculated using Argo data. Dark blue and light blue bars indicate F_{A-S} calculated with and without correction, respectively. Positive F_{A-S} indicates the flux from the atmosphere to the seawater.

increases the sea-to-air O_2 flux (e.g., February and March of Figure 3f). It should be noted that for float f8397 in March (Figure 3b) and float f9306 in January (Figure 3d), applying the skin temperature correction changed the direction of flux from sea-to-air to air-to-sea, which emphasized the importance of such corrections when the surface ocean oxygen was almost in equilibrium with the oxygen in the atmosphere.

As shown in Figure 3, the negative ΔT increases the value of F_{A-S} while the positive ΔT increases the F_{A-S} value, regardless of the sign of F_{A-S}. The more detailed differences in F_{A-S} values with and without the skin temperature correction are presented in Figures 4a–4c. For the subarctic f8397 (Figure 4a) and the subtropical f9306 (Figure 4b), since F_S is mostly dependent on ($[O_2]_{sat}$–[O2]; Equation 3) and ΔT is stronger (further from
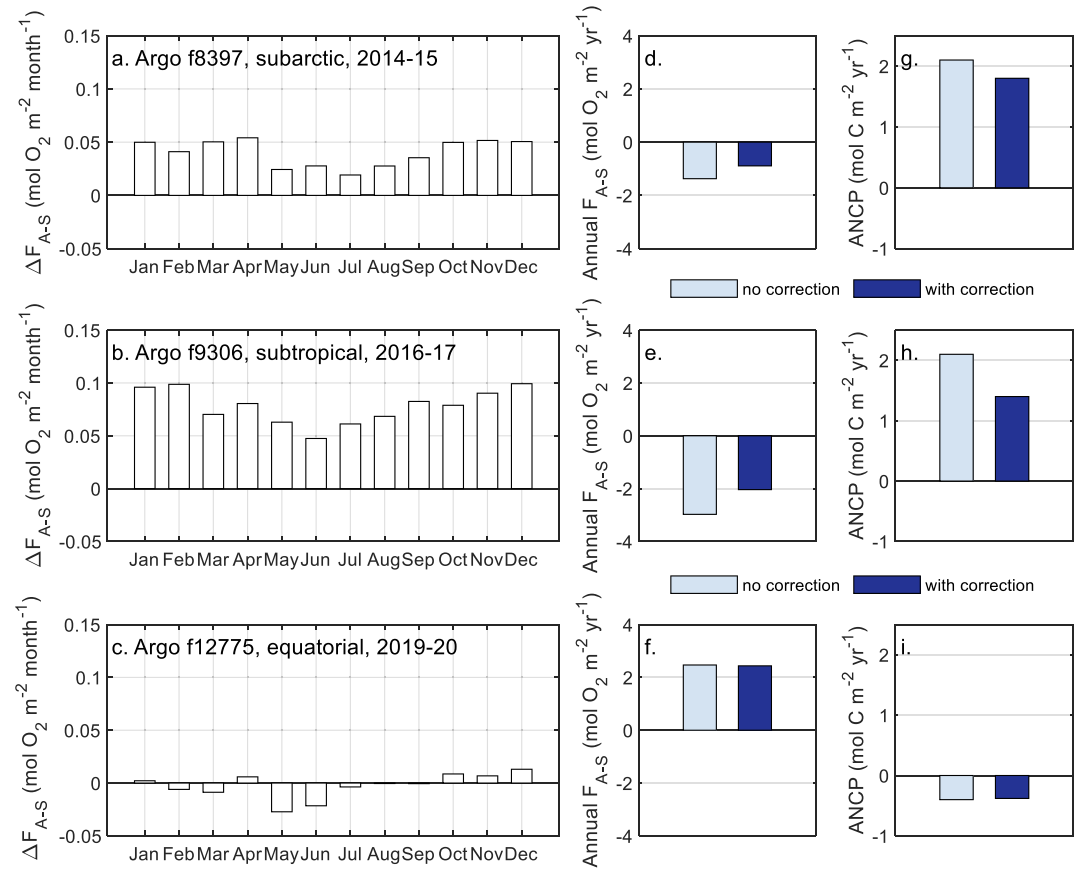
Figure 4. (a–c): Differences in monthly air-sea O_2 flux (ΔF_{A-S}, mol O_2 m^{-2} month^{-1}) calculated with/without skin temperature correction. $\Delta F_{A-S} = F_{A-S\ (\Delta T\ corrected)} - F_{A-S\ (no\ correction)}$ (d–f): Annual (cumulative) air-sea O_2 flux (F_{A-S}, mol O_2 m^{-2} yr^{-1}) calculated with/without skin temperature correction (g–i): Annual net community production (mol C m^{-2} yr^{-1}) calculated with/without skin temperature correction.

zero) in the winter (Figures 3a and 3c), ΔF_{A-S} is larger in the winter. As the correction leads to more positive F_{A-S} values, it consequently decreases F_{NCP} (see Equation 4) and ANCP. The examples from floats f8397 and f9306 with ERA5-based ΔT correction (Table 1) indicate significant changes in F_{A-S} of 0.5 (Figure 4d) and 1.0 (Figure 4e) mol O_2 m^{-2} yr^{-1}, larger than the uncertainty of F_{A-S} estimates (~0.3 mol O_2 m^{-2} yr^{-1}). The differences in F_{A-S} translate into significant ANCP changes of −0.33 mol C m^{-2} yr^{-1} (−16%, Figure 4g) and −0.65 mol C m^{-2} yr^{-1} (−33%, Figure 4h), considering the uncertainties for ANCP estimates in these two regions are ± 0.6 and ±0.3 mol C m^{-2} yr^{-1}, respectively (Yang et al., 2017). The ΔT corrections lead to smaller changes in F_{A-S} and ANCP for the subarctic float f8397 than the subtropical float f9306, because: (a) The absolute value of ΔT is smaller; and (b) the bubble flux (F_B) has larger contribution to F_{A-S} for f8397 (subarctic North Pacific)

Table 1
Annual Air-Sea O_2 Flux (F_{A-S}, Mol O_2 m^{-2} Yr^{-1}) and Annual Net Community Production (ANCP, Mol C m^{-2} Yr^{-1}) Calculated With/Without Skin Temperature Correction

Float	Period	Region	Annual $F_{A-S} = F_S + F_B$ (mol O_2 m^{-2} yr^{-1})		ANCP (mol C m^{-2} yr^{-1})	
			No correction	With correction	No correction	With correction
f8397	2014–15	Subarctic	−1.4 = −2.7 + 1.3	−0.9 = −2.2 + 1.3	2.1	1.8
f9306	2016–17	Subtropical	−3.0 = −3.3 + 0.3	−2.0 = −2.3 + 0.3	2.1	1.4
f12775	2019–20	Equatorial	2.9 = 2.4 + 0.5	2.87 = 2.37 + 0.5	−0.4	−0.38

Note. F_S and F_B are fluxes from diffusion and bubble injection. Positive F_{A-S} indicates the flux from the atmosphere to the seawater.

than for f9306 (subtropical North Pacific), and F_B is not affected by the ΔT correction (Table 1). In contrast, for the equatorial f12775 (Figure 4c), ΔF_{A-S} is much smaller since the ΔT values are closer to zero. ΔF_{A-S} is negative for those months (February, March, May, June, July, and August) when ΔT is positive. Because ΔF_{A-S} oscillates between positive and negative over the course of a year, the over-all effect to the annual (cumulative) F_{A-S} is small ($+0.03$ mol O_2 m^{-2} yr^{-1}, Table 1 and Figure 4f), translating into very small ANCP changes of -0.02 mol C m^{-2} yr^{-1} ($+5\%$, Figure 4i).

4. Summary and Implications

A new approach for the skin temperature correction for air-sea O_2 exchange calculation was created based on the skin temperature and sea surface temperature products from ERA5 reanalysis. The ERA5-derived correction term (ΔT) was consistent to that derived from long-term field measurements at three surface moorings representing a wide range of ΔT values. Our results showed that ΔT has large spatial and temporal variations, and is dominated by the cool skin effect (negative ΔT) in most cases (except for the equatonal region or summertime). Example calculations were carried out with data from three Argo floats in the subarctic, subtropical, and equatorial Pacific. The results show that the skin temperature correction could lead to -1% to $+36\%$ difference in annual air-to-sea O_2 flux, and -33% to $+5\%$ difference in ANCP. Because of the importance of ANCP as a metric of carbon export and the utility of air-sea O_2 fluxes in the calculation of ANCP, it is important to resolve questions about methods presently used to determine the skin temperature and the parameterization of air-sea gas exchange model.

Data Availability Statement

The ERA5 hourly skin temperature (SKT) and sea surface temperature products are from https://cds.climate.copernicus.eu/cdsapp#!/dataset/reanalysis-era5-single-levels?tab=form. The mooring SKT and SST are from https://www.pmel.noaa.gov/ocs/data/fluxdisdel/ and https://www.pmel.noaa.gov/tao/drupal/disdel/. Argo float data is from https://sites.google.com/a/uw.edu/sosargo/home. The Argo data were made freely available by the International Argo Program and the national programs that contribute to it (https://doi.org/10.17882/42182). Wind data is from http://apdrc.soest.hawaii.edu/datadoc/ascat.php.

References

Bushinsky, S. M., & Emerson, S. (2015). Marine biological production from in situ oxygen measurements on a profiling float in the subarctic Pacific Ocean. *Global Biogeochemical Cycles*, *29*, 2050–2060. https://doi.org/10.1002/2015GB005251

Bushinsky, S. M., Emerson, S. R., Riser, S. C., & Swift, D. D. (2016). Accurate oxygen measurements on modified argo floats using in situ air calibrations. *Limnology and Oceanography: Methods*, *14*(8), 491–505. https://doi.org/10.1002/lom3.10107

Cronin, M. F., Fairall, C. W., & McPhaden, M. J. (2006). An assessment of buoy-derived and numerical weather prediction surface heat fluxes in the tropical Pacific. *Journal of Geophysical Research*, *111*, C06038. https://doi.org/10.1029/2005JC003324

Cronin, M. F., & Kessler, W. S. (2002). Seasonal and interannual modulation of mixed layer variability at 0°, 110°W. *Deep Sea Research Part I: Oceanographic Research Papers*, *49*(1), 1–17. https://doi.org/10.1016/S0967-0637(01)00043-7

Cronin, M. F., Pelland, N. A., Emerson, S. R., & Crawford, W. R. (2015). Estimating diffusivity from the mixed layer heat and salt balances in the North Pacific. *Journal of Geophysical Research: Oceans*, *120*(11), 7346–7362. https://doi.org/10.1002/2015JC011010

Donlon, C., Robinson, I., Casey, K. S., Vazquez-Cuervo, J., Armstrong, E., Arino, O., & Rayner, N. (2007). The global ocean data assimilation experiment high-resolution sea surface temperature pilot project. *Bulletin of the American Meteorological Society*, *88*(8), 1197–1214. https://doi.org/10.1175/BAMS-88-8-1197

Donlon, C. J., Martin, M., Stark, J., Roberts-Jones, J., Fiedler, E., & Wimmer, W. (2012). The operational sea surface temperature and sea ice analysis (OSTIA) system. *Remote Sensing of Environment*, *116*, 140–158. https://doi.org/10.1016/j.rse.2010.10.017

Donlon, C. J., Minnett, P. J., Gentemann, C., Nightingale, T. J., Barton, I. J., Ward, B., & Murray, M. J. (2002). Toward improved validation of satellite sea surface skin temperature measurements for climate research. *Journal of Climate*, *15*(4), 353–369. https://doi.org/10.1175/1520-0442(2002)015<0353:TIVOSS>2.0.CO;2

Donlon, C. J., Nightingale, T. J., Sheasby, T., Turner, J., & Emery, W. J. (1999). Implications of the oceanic thermal skin temperature deviation at high wind speed. *Geophysical Research Letters*, *26*, 2505–2508. https://doi.org/10.1029/1999GL900547

Emerson, S., & Bushinsky, S. (2016). The role of bubbles during air-sea gas exchange. *Journal of Geophysical Research: Oceans*, *121*(6), 4360–4376. https://doi.org/10.1002/2016JC011744

Emerson, S., Yang, B., White, M., & Cronin, M. (2019). Air-sea gas transfer: Determining bubble fluxes with in situ N_2 observations. *Journal of Geophysics Research: Ocean*, *124*, 2716–2727. https://doi.org/10.1029/2018JC014786

Fairall, C. W., Bradley, E. F., Godfrey, J. S., Wick, G. A., Edson, J. B., & Young, G. S. (1996). Cool-skin and warm-layer effects on sea surface temperature. *Journal of Geophysical Research*, *101*(C1), 1295–1308. https://doi.org/10.1029/95JC03190

Fairall, C. W., Bradley, E. F., Hare, J. E., Grachev, A. A., & Edson, J. B. (2003). Bulk parameterization of air-sea fluxes: Updates and verification for the COARE algorithm. *Journal of Climate*, *16*, 571–591. https://doi.org/10.1175/1520-0442(2003)016<0571:bpoasf>2.0.CO;2

Garcia, H. E., & Gordon, L. I. (1992). Oxygen solubility in seawater: Better fitting equations. *Limnology & Oceanography*, *37*(6), 1307–1312. https://doi.org/10.4319/lo.1992.37.6.1307

Garcia, H. E., & Gordon, L. I. (1993). Erratum: Oxygen solubility in seawater: Better fitting equations. *Limnology & Oceanography*, *38*(3), 656.

Goddijn-Murphy, L. M., Woolf, D. K., Land, P. E., Shutler, J. D., & Donlon, C. (2015). The ocean flux greenhouse gases methodology for deriving a sea surface climatology of CO_2 fugacity in support of air–sea gas flux studies. *Ocean Science*, *11*(4), 519–541. https://doi.org/10.5194/os-11-519-2015

Hasse, L. (1963). On the cooling of the sea surface by evaporation and heat exchange. *Tellus*, *15*(4), 363–366. https://doi.org/10.1111/j.2153-3490.1963.tb01399.x

Hedges, J. I., Baldock, J. A., Gélinas, Y., Lee, C., Peterson, M. L., & Wakeham, S. G. (2002). The biochemical and elemental compositions of marine plankton: A NMR perspective. *Marine Chemistry*, *78*(1), 47–63. https://doi.org/10.1016/S0304-4203(02)00009-9

Hersbach, H., Bell, B., Berrisford, P., Biavati, G., Horányi, A., Muñoz Sabater, J., et al. (2018). ERA5 hourly data on single levels from 1979 to present. Copernicus Climate Change Service (C3S) Climate Data Store (CDS). https://doi.org/10.24381/cds.adbb2d47

IFS Documentation CY47R1 - Part IV: Physical Processes. (2020). European Centre Medium Range Weather Forecasts. https://doi.org/10.21957/cpmkqvhja

Liang, J. H., Deutsch, C., McWilliams, J. C., Baschek, B., Sullivan, P. P., & Chiba, D. (2013). Parameterizing bubble-mediated air-sea gas exchange and its effect on ocean ventilation. *Global Biogeochemical Cycles*, *27*(3), 894–905. https://doi.org/10.1002/gbc.20080

Luo, B., & Minnett, P. J. (2020). Evaluation of the ERA5 sea surface skin temperature with remotely-sensed shipborne marine-atmospheric emitted radiance interferometer data. *Remote Sensing*, *12*(11), 1873. https://doi.org/10.3390/rs12111873

McGillis, W. R., & Wanninkhof, R. (2006). Aqueous CO_2 gradients for air–sea flux estimates. *Marine Chemistry*, *98*(1), 100–108. https://doi.org/10.1016/j.marchem.2005.09.003

Riser, S. C., & Johnson, K. S. (2008). Net production of oxygen in the subtropical ocean. *Nature*, *451*(7176), 323–325. https://doi.org/10.1038/nature06441

Watson, A. J., Schuster, U., Shutler, J., Holding, T., Ashton, I., Landschützer, P., et al. (2020). Revised estimates of ocean-atmosphere CO_2 flux are consistent with ocean carbon inventory. *Nature Communication*, *11*, 4422. https://doi.org/10.1038/s41467-020-18203-3

Woolf, D. K., Land, P. E., Shutler, J. D., Goddijn-Murphy, L. M., & Donlon, C. J. (2016). On the calculation of air-sea fluxes of CO_2 in the presence of temperature and salinity gradients. *Journal of Geophysical Research: Oceans*, *121*, 1229–1248. https://doi.org/10.1002/2015JC011427

Yang, B., Emerson, S. R., & Bushinsky, S. M. (2017). Annual net community production in the subtropical Pacific Ocean from in situ oxygen measurements on profiling floats. *Global Biogeochemical Cycles*, *31*, 728–744. https://doi.org/10.1002/2016GB005545

Yang, B., Emerson, S. R., & Penã, M. A. (2018). The effect of the 2013-2016 high temperature anomaly in the subarctic Northeast Pacific (the "blob") on net community production. *Biogeosciences*, *15*(21), 6747–6759. https://doi.org/10.5194/bg-15-6747-2018

Yang, B., Emerson, S. R., & Quay, P. D. (2019). The subtropical ocean's biological carbon pump determined from O_2 and $DIC/DI^{13}C$ tracers. *Geophysical Research Letters*, *46*(10), 5361–5368. https://doi.org/10.1029/2018GL081239

Zhang, D., Cronin, M. F., Meinig, C., Farrar, J. T., Jenkins, R., Peacock, D., & Yang, Q. (2019). Comparing air-sea flux measurements from a new unmanned surface vehicle and proven platforms during the SPURS-2 field campaign. *Oceanography*, *32*(2), 122–133. https://doi.org/10.5670/oceanog.2019.220